Observations of the Cosmic Ray Sun Shadow from 1989 to 2001

W.W.M. Allison[3], G.J. Alner[4], D.S. Ayres[1], W.L. Barrett[6], P.M. Border[2], J. Chung[5], J.H. Cobb[3], H. Courant[2], D.M. Demuth[2], T.H. Fields[1], H.R. Gallagher[3], M.C. Goodman[1], R. Gran[2], T. Joffe-Minor[1], T. Kafka[5], S.M.S. Kasahara[2], P.J. Litchfield[4], W.A. Mann[5], M.L. Marshak[2], R.H. Milburn[5], W.H. Miller[2], L. Mualem[2], A. Napier[5], W.P. Oliver[5], G.F. Pearce[4], E.A. Peterson[2], D.A. Petyt[4], K. Ruddick[2], M. Sanchez[5], J. Schneps[5], A. Sousa[5], B. Speakman[2], J.L. Thron[1], S.P. Wakely[2], N. West[3]

[1] *Argonne National Laboratory, Argonne, IL 60439*
[2] *University of Minnesota, Minneapolis, MN 55455*
[3] *Department of Physics, University of Oxford, Oxford OX1 3RH, UK*
[4] *Rutherford Appleton Laboratory, Chilton, Didcot, Oxfordshire OX11 0QX, UK*
[5] *Tufts University, Medford, MA 02155*
[6] *Western Washington University, Bellingham, WA 98225*

PACS: 96.40.Kk, 96.40.Tv, 13.85.Tp

We have measured the cosmic ray shadow of the Sun using 47.8 million muon events recorded by the Soudan 2 deep underground tracking calorimeter between 1989 and 2001. We confirm surface air shower data indicating the shadow varies over the 11-year solar cycle. During a 5-year interval centered on solar minimum solar minimum, the apparent shadow intensity is larger than that expected for a black disk of the same radius as the Sun. The shadow width during these years depends on the presence or absence of sunspots and the shadow shape and size independently depend on the polarity of the Interplanetary Magnetic Field, which changes every few days.

Several high energy cosmic ray detectors, both surface and underground, have observed the cosmic ray shadows of both the Moon and the Sun[1-4]. At TeV and higher energies, the lunar shadow appears well-defined and stable[5]. The Moon shadow is thus useful for calibration of detector angular resolution and pointing. The lunar shadow dispersion of ~5 mr indicates the limited effect of the Earth's geomagnetic field, multiple Coulomb scattering and transverse momentum in production and decay processes on trajectories of high energy cosmic rays. The solar shadow is less defined than the lunar shadow and is variable in time, indicating a measurable dispersion, presumably due to either or both the solar magnetic field and the interplanetary magnetic field (IPMF). The Tibet Air Shower Array has reported a correlation between the solar cosmic ray shadow and the 11-year solar cycle[1], with a centered and more distinct Sun shadow observed during intervals of lower solar activity near the minimum of the solar cycle. Here, we investigate both long interval and few day correlations between the cosmic ray Sun shadow and characteristics of the Sun and the IPMF over an entire solar cycle.

The Soudan 2 detector[6], a 970 metric ton tracking calorimeter originally designed to search for proton decay, has measured deep underground muon events between January 1989 and June 2001. This detector is located 710 m underground in northeastern Minnesota at 47° 49' N. latitude and 92° 14' W. longitude. It consists of 240 modules, each 1 m by 1.1 m by 2.5 m high and containing a steel-plastic-gas honeycomb structure. The overall detector is 8 m by 15 m by 5 m high. The gas is 90% argon-10% carbon dioxide. Ionization electrons are drifted in the gas up to 0.5 m and then proportionally multiplied and collected on thin tungsten wires. The detector measures x,y,z coordinates and dE/dx for all ionizing particle tracks, typically at 30 to 50 points per meter of track length, depending on track orientation, with a uncertainty for each point of ±1 cm in each coordinate. Tracks used for this analysis are typically several meters in length, with a minimum reconstructed track length of 1 m. The arrival time for each event is also recorded, using a clock synchronized to the national time standard.

The cosmic ray data reported here are derived from approximately 10^8 triggers, each representing a deposit of energy above threshold in some local region of the detector. Analysis software attempted to recognize spatial patterns in the data for each triggered event. About half of the triggered events were identified as single or multiple muons. These events were subject to additional cuts to insure that >95% of the accepted events were correctly interpreted and accurately reconstructed. The resultant data sample consists of 47.8 million muon events. Relatively fewer events were recorded between 1989 and 1991, when the detector was still under construction. The number of events then increased slightly from year to year with improvements in detector operating efficiency.

We used for this analysis the daily-averaged IPMF and sunspot data from a public archive maintained by the Goddard Space Flight Center[7]. The IPMF data were mostly measured by spacecraft stationed at the L_1 Lagrangian point, which is approximately 0.01 AU from the earth. The typical magnetic field at this point is 5 nT, with the field lines nearly parallel to the ecliptic or solar equatorial planes[8]. The field lines often lie about 40° from a line connecting the Earth to the Sun because of the solar rotation. The x-component (x axis points from Earth to sun) of the IPMF changes polarity every 7 to 14 days resulting in a 2 to 4 sector structure for the IPMF. The z-component (normal to the ecliptic plane) is typically 1-2 nT. It varies in polarity and its direction is not correlated with the directions of the x and y components. The sunspot number and the magnitude of the IPMF are clearly correlated over the 11-year solar cycle with large numbers of sunspots associated with a large IPMF.

We have analyzed the 47.8 million cosmic ray muon events in order to both test hypotheses about possible cosmic ray shadows and estimate parameters of shadows if they exist. The procedure was as follows. For each event, we calculated the apparent direction of the Moon and Sun at the event arrival time. We then determined the angle θ between the muon direction and the direction of the Moon or Sun. Events pointing within 5° of each of these objects were aggregated into binned histograms of $dN/d\Omega$ vs. θ, where $d\Omega$ is the usual solid angle, $d\Omega = 2\pi \sin\theta \, d\theta$. We then performed maximum likelihood fits of $dN/d\Omega$ to the sum of a Gaussian shadow function centered at $\theta = 0°$ and a constant background, that is $\frac{dN}{d\Omega} = \lambda\left[1-\left(\frac{r^2}{2\sigma^2}\right)e^{-\frac{\theta^2}{2\sigma^2}}\right]$.

The parameter λ measures flux and exposure and is not interesting for analysis of a possible cosmic ray shadow. The parameter r is the radius of a "black disk" that absorbs an equal flux to that absorbed by a Gaussian shadow with variance σ^2. For the Moon shadow, σ^2 can be partitioned into two sub-variances, that is, $\sigma^2 = \sigma_o^2 + \sigma_d^2$, where σ_o^2 is the variance due to the finite size of the Moon and σ_d^2 is the variance due to finite detector angular resolution, dispersion by the Earth's geomagnetic field, multiple Coulomb scattering and hadronic production. For the Sun shadow, $\sigma^2 = \sigma_o^2 + \sigma_d^2 + \sigma_x^2$, where σ_o^2 and σ_d^2 are identical in definition and value to these parameters in the Moon shadow function. σ_x^2 is the additional variance in the shadow function due to the Sun's magnetic field and the IPMF. For a "black disk," $\sigma_o^2 = r^2/2 = 0.0313\ (°)^2$ for the Sun and Moon (both objects have an angular radius of 0.25° as viewed from the Earth). We estimate $\sigma_d^2 = 0.0547\ (°)^2$ from the Moon shadow as described below. For each shadow, we report (Table 1) r, the equivalent "black disk" radius and $\sigma_x^2 = \sigma^2 - \sigma_o^2 - \sigma_d^2 = \sigma^2 - 0.0860\ (°)^2$, the variance due to the Sun and the IPMF. We test the validity of each likelihood fit using the usual χ^2 test (Table 1). We test the probability that a shadow is preferred by the data to no shadow (H_0) or that one shadow function is preferred to another shadow function (H_1) by a difference in the likelihood function L, that is Prob (H) = Prob ($\chi^2 > 2\Delta L$, 2 dof).[9]

Fig. 1 shows the observed Moon and Sun shadow for the entire data sample from 1989 to 2001, with each plot fit by a Gaussian shadow function plus background. Though the Moon and the Sun are of the same angular size as viewed at the earth, the cosmic ray shadows for the two bodies are clearly different. (The Moon shadow is plotted with 0.1° bins to more clearly show its angular width.) The much narrower Moon shadow indicates that the ~0.6° angular width of the solar shadow results from either or both the Sun and the IPMF. We determine $\sigma_d = (0.234\text{-}0.035\text{+}0.051)°$ by fitting the Moon shadow in Fig. 1a, using fixed values of r = 0.25° and $\sigma_o = r/2$. The probability for this fit using a χ^2 test is 0.69. The probability that the Moon data are consistent with no shadow is 2.1×10^{-7}. We then fit the Sun shadow in Fig. 1b using λ, r and σ_x as free parameters. The results of these fits, listed in Table 1, suggest that for the aggregated Sun shadow data, the shadow intensity (as measured by r, the "black disk" radius) is consistent with the geometric size of the Sun, while σ_x, the width due to the Sun and IPMF, is 0.47°. The probability that the Sun data are consistent with no shadow is 2.2×10^{-2}.

The plots in Fig. 2 investigate the relationship between the Sun shadow observed in deep underground muons and the solar cycle. The solar cycle results in a modulation of both the solar and interplanetary magnetic fields. The cycle is most easily observed in terms of daily sunspot numbers and monthly averages of daily sunspot numbers. The last two solar sunspot maxima, measured by monthly averages, occurred in August 1990 and July 2000. The last minimum in solar sunspot activity was observed in October 1996. Forty-eight percent of the muons observed by the Soudan 2 detector were recorded during the years 1994 through 1998. We associate those years with lesser solar activity and the remainder of the data sample with greater solar activity. Fig. 2(a) shows the plot of $dN/d\Omega$ vs. θ for the years 1994-1998, which we describe as the low solar activity sample. As indicated by the fit parameters listed in Table 1, this shadow has both a higher intensity and a larger variance than the aggregate shadow shown in Fig. 1(b). Fig. 2(b) shows the same plot for the years 1989-1993 and 1999-2001, the high solar activity sample. These data are just the complement of those in Fig. 2(a) and are consistent (9% probability) with no shadow at all (H_0). The probability that the data in Figs. 2(a) and 2(b) are derived from the same distribution (H_1) is 2.1×10^{-3}. These data support the hypothesis of variation of the cosmic ray Sun shadow over the solar cycle. They further suggest that, near solar minimum, the shadow has more than three times the area of the sun, while near solar maximum, the shadow almost disappears.

The larger intensity of the shadow near solar minimum facilitates a study of possible short-term variations in the characteristics of the Sun shadow. One type of short-term variation is the number of sunspots. For 300 days during the years 1994 through 1998, there were zero visible sunspots (19 days in 1994, 58 in 1995, 159 in 1996, 61 in 1997 and 3 in 1998). These no sunspot days occur in groups of several days at a time separated by days with sunspots. Because sunspots are associated with disturbances on and near the solar surface, we speculated that the Sun shadow might be spread by this turbulence. On days with no sunspots, the spread of the shadow might be minimal. Fig. 2(c) shows the plot of $dN/d\Omega$ vs. θ for days with no sunspots. A comparison between this plot and Fig. 2(a), suggests that the spread of the shadow is indeed narrower on the days with no sunspots, while the intensity of the shadow, as measured by r, is similar to the intensity on other days during 1994-1998. This observation has several caveats. (1) Because of limited numbers of events on days with no sunspots, there is a 3% probability that Figs. 2(c) and its complement, that is, the shadow on days with sunspots (not shown) are actually drawn from the same parent distribution. (2) As indicated above, the days with no sunspots are clustered near solar minimum and not evenly spread throughout 1994-1998. It is possible that any differences between Figs. 2(c) and its complement result from proximity to solar minimum, although the year-by-year shadows for days with sunspots do not suggest such an effect.

A second type of short-term variation is possible modulation of the Sun shadow by the polarity of the IPMF. This IPMF polarity in the ecliptic plane alternates every 7 to 14 days. The IPMF polarity normal to the plane changes on a similar timescale and is uncorrelated with the in-plane polarity. Although the magnitude of the IPMF is correlated with sunspot number, there is no relationship between the polarity of the IPMF and the total sunspot number. Indeed, because it is not clear how the IPMF polarity might affect the Sun's cosmic ray shadow, our *a priori* hypothesis was that Sun shadow characteristics should not be unaffected by IPMF polarity. We decided to separately determine the appearance of the shadow for positive and negative B_x and B_z, where B_x is the IPMF component parallel to the Earth-Sun line ($B_x > 0$ is towards the Sun) and B_z is the component perpendicular to the ecliptic plane ($B_z > 0$ is towards the Earth's north pole). Figs. 3(a) and 3(b) show the plots of $dN/d\Omega$ vs. θ for the years 1994-1998 for $B_x < 0$ and $B_x > 0$, respectively. Figs. 3(c) and 3(d) show the same plots for $B_z < 0$ and $B_z > 0$, respectively.

The plots in Fig. 3 qualitatively suggest a dependence of the Sun shadow on the IPMF polarity. For $B_x < 0$, that is IPMF pointing towards the Earth, the shadow is narrower and smaller. For $B_x > 0$, IMPF pointing towards the Sun, the shadow is more intense and wider. Indeed, the shadow in Fig. 3(a) is as narrow as the Moon shadow in Fig. 1(a) and the fit is consistent with $\sigma_x = 0$. The shadow also appears to depend on the polarity of B_z. The shadow is clearly defined when the IPMF points south of the ecliptic plane, but the data appear consistent with no shadow when the IPMF points north of the ecliptic plane. The parameters for the Gaussian shadow fits are listed in Table 1. A likelihood test for the consistency of Figs. 3(a) and 3(b) indicates a probability of 1.8×10^{-4}. The likelihood test is more ambiguous for Figs. 3(c) and 3(d) indicating a chance probability of 0.04 that the data in these two figures are drawn from the same parent distribution. We know of no models that relate the cosmic ray Sun shadow to the polarity of the IPMF, although it is possible that some interaction between the IPMF and either the Sun's magnetic field or the geomagnetic field leads to the effects we observe.

The data presented here indicate that the Sun's cosmic ray shadow is variable. The shadow is clearly more intense and larger during the years near solar minimum. During this period, distinct modulations occur on timescales of a few days, correlated with changes in the sunspot number and the orientation of the IPMF. The effective angular area of the solar disk varies from nearly zero to more than five times that size on days near solar minimum, when the IPMF points towards the Sun. These data suggest that cosmic rays may be an effective probe of the solar magnetosphere, although a detector area larger than the size of the Soudan 2 detector is likely required to measure the Sun shadow on a near real-time basis.

This work was supported by the U.S. Department of Energy, the U.K. Particle Physics and Astronomy Research Council, and the State and University of Minnesota. We wish to thank the Minnesota Department of Natural Resources for allowing us to use the facilities of the Soudan Underground Mine State Park.

References

[1] M. Amenomori, *et al.*, Astrophys. J. **541**, 1051 (2000); Adv. In Space Res. **23**, 611 (1999); Astrophys. J. **464**, 954 (1996); Astrophys. J. Lett. **415**, L147 (1993); Phys. Rev. **D47**, 2675 (1993).

[2] A. Borione, *et al.*, Phys. Rev. **D49**, 1171 (1994).

[3] D.E. Alexandreas, *et al.*, Phys. Rev. **D43**, 1735 (1991).

[4] M. Ambrosio, *et al.*, Phys. Rev. **D59**, 012003 (1999).

[5] J.H. Cobb, *et al.*, Phys. Rev. **D61**, 092002 (2000).

[6] W.W.M. Allison, *et al.*, Nucl. Inst. Meth. **A381**, 385 (1996) and **A376**, 36 (1996).

[7] http://nssdc.gsfc.nasa.gov/omniweb/ow.html

[8] E.N. Parker, *Cosmical Magnetic Fields*, Clarendon Press, Oxford, 1979.

[9] G. Cowan, *Statistical Data Analysis*, Oxford University Press, Oxford, 1998, p. 89.

Figure Captions

Fig. 1—The cosmic ray shadows of the (a) Moon and the (b) Sun plotted as $dN/d\Omega$ vs. θ for the years 1989 through May, 2001. Angular bins of 0.1° are used for the Moon because of the sharpness of its shadow. The angular bins for the Sun are 0.2°.

Fig. 2—The cosmic ray shadow of the Sun plotted as $dN/d\Omega$ vs. θ for the years (a) 1994 through 1998, years are associated with a minimum of solar activity, (b) 1989-1993 and 1999-2001, years associated with maximal solar activity. Fig. 2(c) shows the Sun shadow for days with no sunspots, all of which occurred during the interval 1994-1998.

Fig. 3—The cosmic ray Sun shadow aggregated for 1994-1998 in four subsets depending on the daily average value of the Interplanetary Magnetic Field. The x-component of the field (a,b) lies along the Sun-Earth line (positive x towards the Sun). The z-component of the field (c,d) is

normal to the ecliptic plane (positive z towards the North). The shape of the Sun shadow appears dependent on the IPMF polarity.

Table 1. Estimates of the parameters of the Gaussian shadow functions derived from the fits described in the text.

Figure	Conditions	*r*	-	+	σ_x	-	+	χ^2/df
1(a)	Moon	0.243	0.032	0.033				41.8/47
1(b)	Sun	0.256	0.065	0.069	0.47	0.16	0.37	25.2/22
2(a)	Sun 94-98	0.44	0.10	0.17	0.80	0.21	0.76	23.8/22
2(b)	Sun 89-93,99-01	*						33.9/24
2(c)	Sun, $N_{sunspots} = 0$	0.43	0.10	0.10	0.27	0.20	0.26	21.5/22
3(a)	Sun, 94-98, $B_x < 0$	0.22	0.05	0.06	0		0.23	23.0/22
3(b)	Sun, 94-98, $B_x > 0$	0.60	0.13	0.10	0.82	0.17	0.37	16.8/22
3(c)	Sun, 94-98, $B_z < 0$	0.43	0.09	0.09	0.51	0.16	0.26	25.0/22
3(d)	Sun, 94-98, $B_z > 0$	*						20.1/22

* $dN/d\Omega$ vs. θ is consistent with no shadow, which precludes reliable estimates of parameters and their uncertainties.

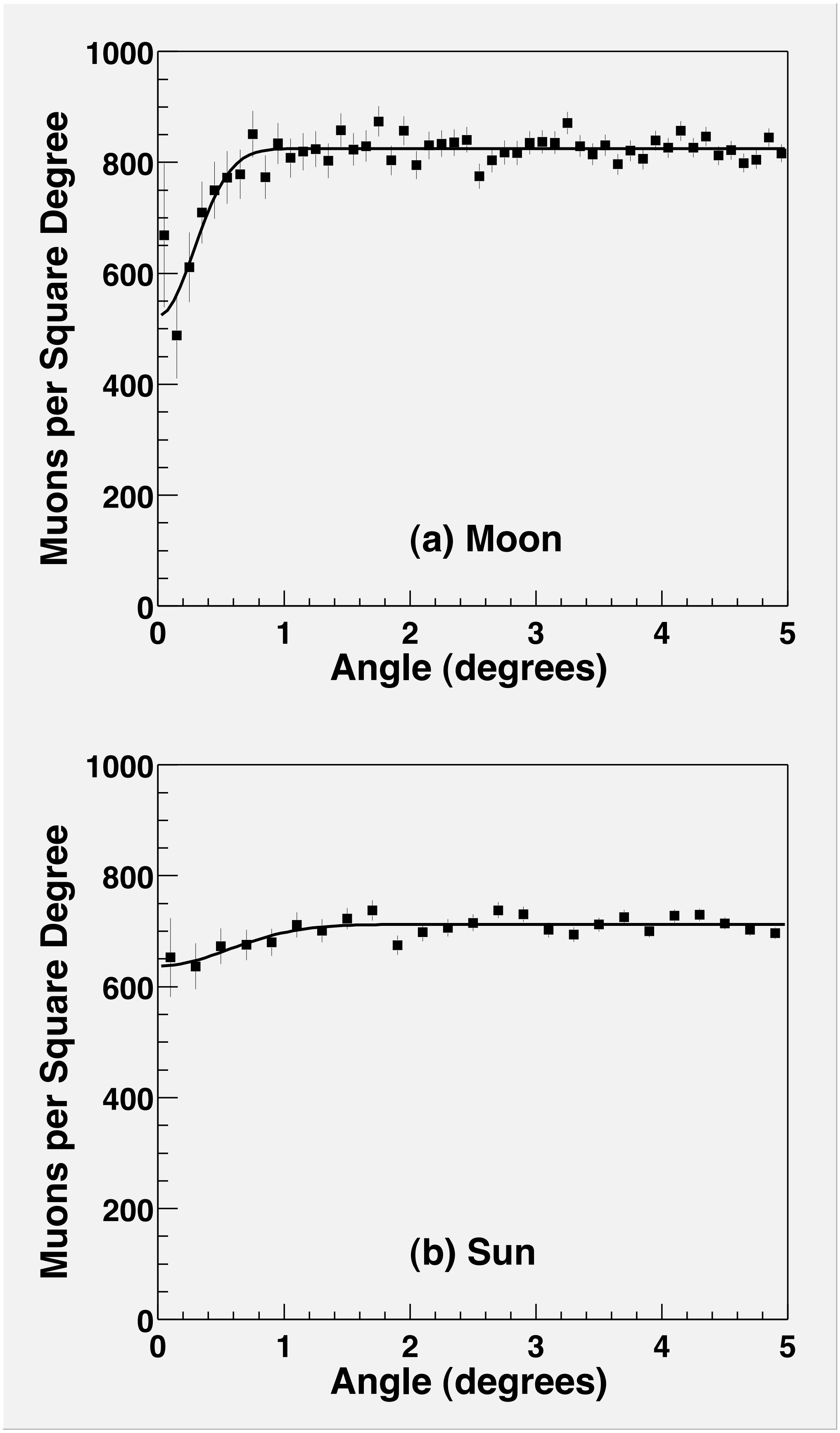
1000
800
600
400
200
0
Muons per Square Degree
(a) Moon
0
1
2
3
4
5
Angle (degrees)
1000
800
600
400
200
0
Muons per Square Degree
(b) Sun
0
1
2
3
4
5
Angle (degrees)

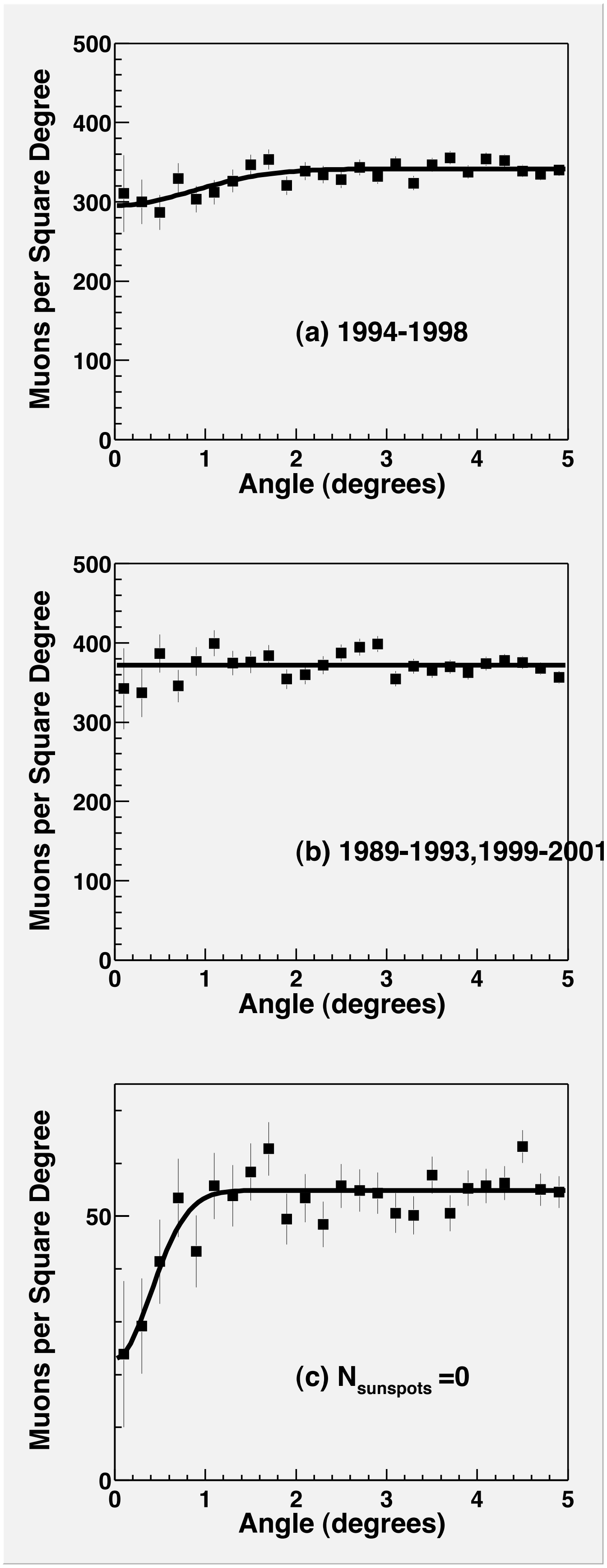
Muons per Square Degree
500
400
300
200
100
0
0
1
2
3
4
5
Angle (degrees)
(a) 1994-1998
Muons per Square Degree
500
400
300
200
100
0
0
1
2
3
4
5
Angle (degrees)
(b) 1989-1993,1999-2001
Muons per Square Degree
50
0
0
1
2
3
4
5
Angle (degrees)
(c) $N_{sunspots}$ =0

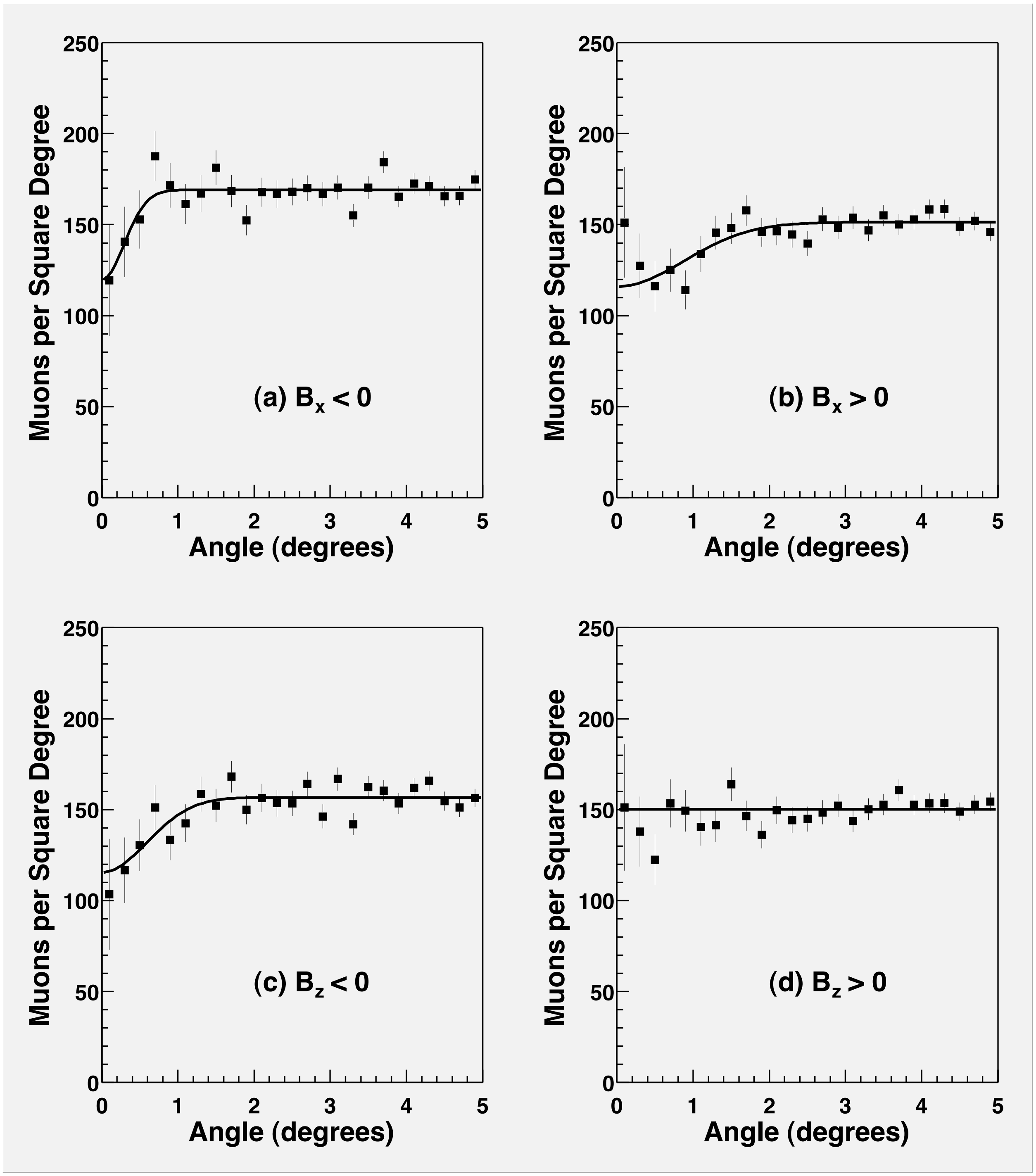
(a) $B_x < 0$
(b) $B_x > 0$
(c) $B_z < 0$
(d) $B_z > 0$
Muons per Square Degree
Angle (degrees)
0
50
100
150
200
250
0
1
2
3
4
5